Phase behavior and molecular mobility of *n*-octylcyanobiphenyl confined to molecular sieves: Dependence on the pore size

Ligia Frunza,[1,*] Stefan Frunza,[1] Hendrik Kosslick,[2] and Andreas Schönhals[3]
[1]*National Institute of Materials Physics, R-077125 Magurele, Romania*
[2]*Leibniz Institute for Catalysis at the University of Rostock, D-18059 Rostock, Germany*
[3]*Federal Institute for Materials Research and Testing (BAM), D-12205 Berlin, Germany*
(Received 27 June 2008; published 3 November 2008)

The molecular dynamics of 4-*n*-octyl-4′-cyanobiphenyl (8CB) confined inside the pores of a series of AlMCM-41 samples with the same structure, constant composition (Si/Al=14.7) but different pore sizes (diameter between 2.3 and 4.6 nm) was investigated by broadband dielectric spectroscopy (10^{-2}–10^{9} Hz) in a large temperature interval. Two relaxation processes are observed: one has a bulklike behavior and is assigned to the 8CB in the pore center. The relaxation time of the second relaxation process is essentially slower than that of the former one and this process is related to the dynamics of molecules in a surface layer with a paranematic order. Both relaxation processes are specifically influenced by the interaction of the molecules with the surface and by the confinement. Above the clearing temperature the temperature dependence of the relaxation rate of the bulklike process obeys the Vogel-Fulcher-Tammann (VFT) law. The Vogel temperature increases with decreasing pore size. This is explained by increasing influence of paranematic potential of the surface layer with decreasing pore size. The temperature dependence of the relaxation rate of the surface layer follows also the VFT formula and the Vogel temperature decreases with decreasing pore size. This temperature dependence is controlled by both the interaction of the 8CB molecules with the surface via hydrogen bonding and by spatial confinement effects. To discriminate between both effects the data for the surface layer of 8CB confined to the molecular sieves are compared with results concerning 8CB adsorbed as a quasimonolayer on the surface of silica spheres of aerosil. On this basis a confinement parameter is defined and discussed.

DOI: 10.1103/PhysRevE.78.051701 PACS number(s): 61.30.Pq, 61.30.Hn, 64.70.pp, 82.75.−z

I. INTRODUCTION

The behavior of molecules confined to restricted geometries on the nanometer scale has received a considerable attention especially from the theoretical point of view during the recent years [1–4]. This growing interest is due to finite size effects and of quenched disorder of soft condensed matter including super fluids, random magnets, elastomers, and liquid crystals[4,5].

Molecular sieves are suitable as confining hosts due to their arrays of pores and cavities with known geometries, high internal surface area, and chemical as well as mechanical stability [1,6–10]. In general the structure and the molecular dynamics of matter in nanoconfinements are due to a counterbalance of surface and finite size effects. The relative influence of the interaction of the molecules with the surface (surface anchoring of molecules) and finite size effects is determined by the size of the pores and by the strength of this interaction: Finite size effects should dominate if the pore size is small [11]. It is also expected that confinement and disorder have a considerable influence on the molecular mobility and therefore on the relaxation processes as well, yielding to a change of the bulklike behavior. Moreover, due to the interaction of the molecules with the surface new structures can be established. Relaxation spectroscopy such as broadband dielectric techniques can be applied to study this confinement and interaction induced structures where relaxation processes, which are not characteristic for the bulk system are observed. These processes are, for instance, due to fluctuations of molecules adsorbed onto the pore surface forming a surface layer. Recently it was demonstrated that the molecular dynamics of these adsorbed molecules resemble some properties, which are characteristic for glassy dynamics [7,12,13].

In this contribution, results concerning the reorientational fluctuations of 4-*n*-octyl-4′-cyanobiphenyl (8CB) confined inside the pores of a series of AlMCM-41 type molecular sieves are reported. These molecular sieves have the same chemical composition and a hexagonal structure of cylindrical pores. The pore diameter varies from 2.3 to 4.6 nm with a rather narrow pore size distribution. Dielectric spectroscopy in a broad frequency and temperature range was applied to investigate the complex dynamical behavior of 8CB molecules confined inside the pores of these molecular sieves. The obtained results are parametrized by the relaxation rate and strength, which are discussed in dependence on the pore diameter in comparison to the bulk. Comparison is made for 8CB confined to other host systems as well.

II. EXPERIMENTAL

8CB was chosen as guest molecule because it is thermally stable. In the bulk 8CB forms liquid crystalline phases with the well-known phase transitions

$$294.4\ \mathrm{K}(Cr/S_A),\quad 306.7\ \mathrm{K}(S_A/N)\ \text{and}\ 314\ \mathrm{K}(N/I),$$

where *Cr* symbolizes the crystalline, S_A the smectic *A*, *N* the nematic, and *I* the isotropic state. 8CB was purchased from

*lfrunza@infim.ro

TABLE I. Texture properties of the AlMCM-41 samples.

Sample	BET Area $[m^2/g]$	Pore diameter d [nm]	Pore volume $[cm^3/g]$
M23	692	2.3	0.911
M28	868	2.8	0.788
M30	979	3.0	0.598
M36	896	3.6	0.978
M46	651	4.6	0.917

Aldrich and was used without further purification.

Molecular sieves of MCM-41 type, with molar ration Si/Al=14.7, were hydrothermally prepared starting from a modified known recipe [14]. The synthesis gels have the same molar composition [15,16]. Alkyltrimethylammonium chloride with alkyl chains of 12 to 18 carbon atoms as template allowed to tune the pore sizes. The materials were transformed into the hydrogen form of the corresponding molecular sieve [16]. Afterwards, they were routinely characterized by x-ray diffraction and electron microscopy, which gives a rather uniform pore structure of hexagonally ordered cylindrical pores. The texture features obtained by nitrogen absorption are presented in Table I. The sample labels carry the value of the mean pore diameter in Å. The pore size distribution is narrow in the case of the samples M23, M28, and M30 and less narrow in the case of the samples with larger pores.

Finely grounded powder of these molecular sieves was pressed under a low pressure to self-supported pellets with a thickness of around 100 μm. To remove water and other impurities adsorbed at the pore walls the pellets were evacuated under vacuum (10^{-5} mbar) at 573 K for 8 h. After that the pores of the molecular sieves are loaded with 8CB using a solution route [17,18]. 8CB was solved in acetone (around 0.5 mol/L) and the pellets of the molecular sieves were immersed in this solution in small excess. The samples were kept in contact with that solution for 6 h at room temperature. After that the solvent was firstly evaporated, and then the excess of the 8CB molecules located on extra pores of the grains and on the outer surface of the molecular sieves were removed as much as possible by applying a low vacuum (10^{-2} mbar) at 373 K for at least 1 h to the sample. The removal of the excess 8CB was checked optically when the optical state of the sample changes from translucent to opaque.

The loading or filling degree of 8CB inside the pores was estimated by thermogravimetric (TG) measurements as already described for other composites [19]. The weight loss due to the decomposition and burning of the organic part is measured up to around 723 K while the molecular sieve are thermally stable up to essentially higher temperatures (its weight is constant by increasing the temperature up to 1073 K). The thermogravimetric measurements were performed by a Setaram TG-DTA 92 apparatus, under a dry nitrogen atmosphere, using a part of the sample prepared for the dielectric measurements and a heating rate of 10 K/min. The content of 8CB c_{8CB} was determined and the loading degree $\Theta = c_{8CB}/(V_{pores}\rho_{8CB}^{conf})$ was estimated by assuming for the density of confined 8CB the same value as in the bulk $\rho_{8CB}^{conf} \approx 1$ g cm^{-3}. The samples were further labeled as 8CB/Mx where Mx is the corresponding molecular sieve (see Table I). The samples were prepared just before the measurements and handled in a desiccator.

The equipment to measure the complex dielectric function $\varepsilon^*(f) = \varepsilon'(f) - i\varepsilon''(f)$ (f: frequency, ε': real part, ε'': loss part) in the frequency range from 10^{-2} to 10^9 Hz was described in detail elsewhere [20(a)]. For frequencies from 10^{-2} to 10^6 Hz a Schlumberger 1260 frequency response analyzer supplemented by a buffer amplifier of variable gain was used whereas for frequencies between 10^6 and 10^9 Hz a coaxial reflectometer using the HP 4191A device was employed. For the former equipment the typical accuracy in $\tan\delta = \varepsilon''/\varepsilon'$ is 10^{-3} because the capacity is low; for the reflectometer it is 10^{-2}.

The dielectric measurements were carried out under isothermal conditions where the temperature was controlled by custom made nitrogen gas jet heating systems. The temperature was increased stepwise from 220 to 428 K in order to cover the temperatures where 8CB is in the crystalline state, all its phase transition temperatures and temperatures in the isotropic state of bulk 8CB as well. The stability of the temperature is better than 0.1 K.

The model function of Havriliak-Negami (HN) function is used to analyze and to separate the different relaxation processes (details can be found in Ref. [20(b)]). The HN function reads

$$\varepsilon^*(f) - \varepsilon_\infty = \frac{\Delta\varepsilon}{[1 + (if/f_0)^\beta]^\gamma}, \tag{1}$$

where f_0 is a characteristic frequency related to the frequency of maximal loss f_p (relaxation rate), ε_∞ describes the value of the real part ε' for $f \gg f_0$. β and γ are fractional form parameters ($0 < \beta \leqslant 1$ and $0 < \beta\gamma \leqslant 1$) characterizing the shape of the relaxation time spectra. $\Delta\varepsilon$ denotes the dielectric strength, which is proportional to the mean square of the effective dipole moment and to the number of the fluctuating dipoles per unit volume. Conduction effects are treated in the usual way by adding a conductivity contribution $\sigma_0/\varepsilon_0(2\pi f)^s$ to the dielectric loss where σ_0 is related to the dc conductivity of the sample and ε_0 is the dielectric permittivity of vacuum. The parameter s ($0 < s \leqslant 1$) describes for $s < 1$ non-Ohmic effects in the conductivity. For details see Refs. [20(b),16]. The results obtained for bulk 8CB were compared with those of 8CB confined to the molecular sieves using mainly the temperature dependence of the relaxation rate f_p and partly that of the dielectric strength $\Delta\varepsilon$.

The interaction of the 8CB molecules with the pore surface of molecular sieves is investigated by Fourier transform infrared (FTIR) spectroscopy measurements with a resolution of 2 cm^{-1} as described previously [9].

III. RESULTS AND DISCUSSION

Information about the filling degree of 8CB in the AMCM-41 molecular sieves was obtained from thermo-

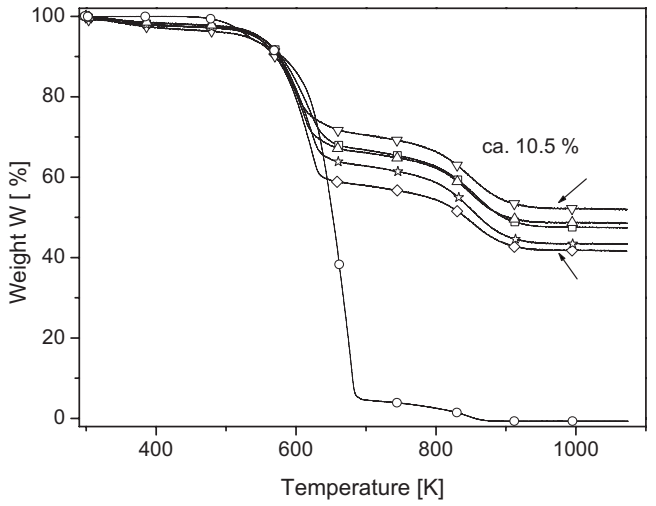

FIG. 1. TG curves for the different samples: ☆-8CB/M23, △-8CB/M28, ◇-8CB/M30, ▽-8CB/M36, □-8CB/M46. The behavior of bulk 8CB (○) was given for comparison.

gravimetric data. Figure 1 shows that all samples have a similar mass loss. The changes are in a rather narrow interval of around 10%, which allows a direct comparison of the samples. In addition to that, the data show that bulk and confined 8CB thermally decompose in a similar manner: The small differences might indicate the interaction of the molecules with the surface in the composite systems.

The filling degree calculated on the basis of the TG data is given in Table II. The obtained values are close to that expected for completely filled pores.

The FTIR spectra indicate that the 8CB molecules interact strongly with the pore surface of the molecular sieves (Fig. 2). The peaks in the FTIR spectra were assigned as already described (e.g., Ref. [9]). The main CN stretching peak was separated into two Gaussian curves. One contribution is centered at 2226 cm^{-1} with a weak intensity. A peak at 2226 cm^{-1} characteristic to CN stretching is also observed for bulk 8CB, which means that, a small part of the confined

TABLE II. Loading degree of the composites.

Sample	8CB/dry molecular sieve %
8CB/M23	88.7
8CB/M28	94.7
8CB/M30	88.6
8CB/M36	105.7
8CB/M46	101.2

8CB is in a bulklike state [9]. The second contribution at 2236 cm^{-1} is much more intense and rather broad. This indicates that the main part of the molecules is in a strong interaction with the surface via the CN group of 8CB and the free surface hydroxyl groups of the molecular sieves. The involvement of the latter in the H bonding with the 8CB molecules is also confirmed by the FTIR spectra in the region of OH stretching.

The strong interaction of the 8CB molecules with the pore surfaces leads to a formation of a surface layer with a structure different of that of bulk 8CB. But the strong anchoring of the cyanobiphenyl (CB) molecules leads to a surface induced order of these molecules, which can be described as a local paranematic state. This was already observed for *n*-alkyl-cyanobiphenyls confined to pores [6,7] and for their composites with aerosil for a broad range of silica densities [18]. Due to the strong interaction the surface induced order persists for temperatures higher than the clearing temperature of the bulk CB (isotropic state) but decreases with increasing the distance from the surface.

The dielectric properties of bulk 8CB have been known for a long time [20(c),21–23]. In the liquid crystalline state due to its anisotropic structure several relaxation process are observed which are predicted also theoretically [20(c)]. The relaxation mode at the lowest frequencies is due to rotational fluctuations of the molecule around its short axis (δ relaxation). In addition to this process, there are three other relax-

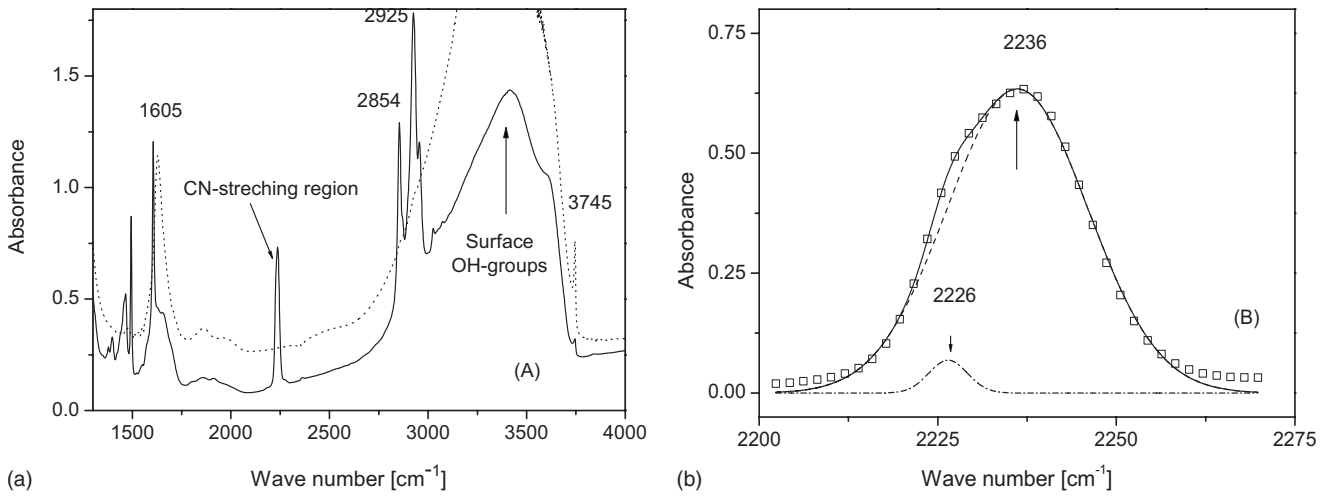

FIG. 2. (A) FTIR spectrum of the sample 8CB/M36 (solid line) and for the empty molecular sieve M36 (dotted line). (B) FTIR spectrum for the CN-stretching vibration (□) for 8CB/M36 together with the Gaussian fits for bulklike 8CB (dashed-dotted line) and confined 8CB (dashed line). The solid line is the whole fit function.

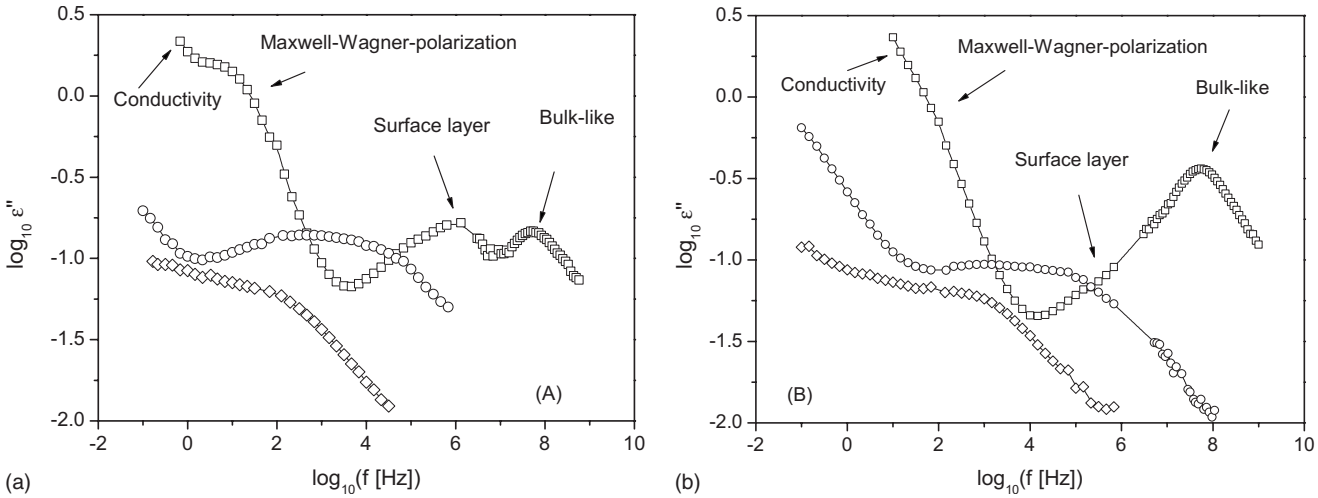

FIG. 3. Dielectric loss vs frequency for 8CB confined to two molecular sieves. (A) 8CB confined to M23. □: $T=329$ K, ○: 268 K, ◇: 234 K. The lines are guides to the eyes. (B) 8CB confined to M46. □: $T=331$ K, ○: 270 K, ◇: 240 K. The lines are guides to the eyes.

ation modes (different tumbling modes of the molecules around their long axis), which have nearly the same relaxation rate and form a broad relaxation process observed at higher frequencies than the δ relaxation. Recent theories predict a further relaxation process related to fluctuations of the molecules on a cone around the director [23]. Above the clearing temperature $T_{N/I}$ the two processes collapse into one broadened relaxation.

Considering these theoretical approaches [20(c)] the temperature dependence of the relaxation rates for both the δ relaxation and the tumbling modes should obey the Arrhenius law

$$f_p = f_\infty \exp[-E_A/(k_B T)] \tag{2}$$

(E_A: activation energy, f_∞: pre-exponential factor, k_B: Boltzmann's constant, T: temperature). But measurements performed over a large temperature interval have shown that this dependence probably obeys the Vogel-Fulcher-Tammann (VFT) law [20(d)] in both the isotropic and the liquid crystalline state as well [22,24–27]. The VFT formula reads

$$\log_{10} f_p = \log_{10} f_\infty - \frac{A}{T - T_0}, \tag{3}$$

where f_∞ and A are constants. T_0 is the so-called Vogel temperature [20(b)].

For the comparison of the molecular dynamics of 8CB in the bulk and in confinement only the δ relaxation is further considered. The dielectric spectra of unloaded AlMCM-41 samples do not show any dielectric loss process and moreover the absolute level of the dielectric loss is low. So it is proven that the contribution of the pore wall material (motions of the silica or alumina tetrahedra as building groups) is negligibly small compared to that observed for the (liquid) filled samples [7].

The dielectric properties of 8CB molecules will be influenced by at least two effects. On the one hand, the structure of MCM-41 molecular sieves consists of randomly oriented grains having cylindrically shaped unidirectional oriented pores with a narrow radii distribution. There is an inherent randomness due to the grain orientation; therefore it is expected that their local orientation has an overall randomizing effect on the nematic director (preferred alignment direction) of confined 8CB. This is known as quenched disorder. On the other hand, the molecules, which are adsorbed at the pore walls, can fluctuate in the surface layer. Generally, in dependence of the pore size different relaxation processes are expected. In Fig. 3 the dielectric loss ε'' versus frequency is shown in the available frequency range as function of temperature for 8CB confined to molecular sieves of two different pore sizes [Fig. 3(a)—2.3 nm, Fig. 3(b)—4.6 nm]. Two relaxation processes are observed indicated by peaks in the dielectric loss.

For all the molecular sieves the process at lower frequencies is assigned to the reorientational dynamics of molecules located in a surface layer whereas the peak observed for higher frequencies is ascribed to 8CB situated in the center of the pores (bulklike 8CB). It is worth noting that for the sample with the larger pore size the relative intensity of the bulklike process is higher than for the lower pore size as expected. At lower frequencies the dielectric spectra show a Maxwell-Wagner-Sillars phenomenon due to the blocking of charge carriers at boundaries and a conductivity contribution. For the smaller pore size the Maxwell-Wager-Sillars process is more pronounced than for the larger one as also expected.

Figure 4 gives the dielectric loss of 8CB confined to the molecular sieves M23 for two different temperatures together with an example for the evaluation strategy used. Due to the presence of two relaxation processes related to a bulklike behavior and that due to the fluctuations of the molecules in a surface layer a sum of two HN functions were fitted to the data. The contribution related to the surface layer to the whole dielectric loss is also given in the figure. The inset of the figure gives the same for 8CB confined to M46 for one temperature.

The frequency of maximum dielectric loss f_p is plotted versus inverse temperature for the sample 8CB/M46 in Fig. 5. The temperature dependence of the relaxation rate for the δ relaxation of bulk 8CB is given for comparison. In the

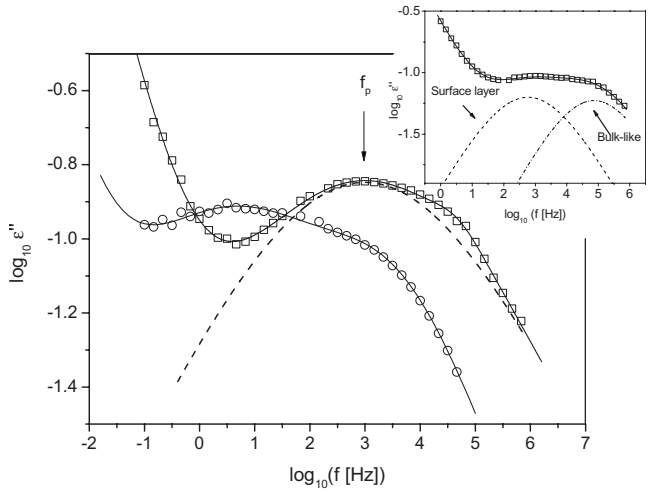

FIG. 4. Dielectric loss ε'' vs frequency for 8CB confined to the molecular sieve M23 for two different temperatures. □: $T=271.5$ K, ○: $T=253$ K. The solid line is the whole fit function as a sum of two HN functions to the data. The dashed line presents the contribution of the surface layer for $T=271.5$ K. The inset gives the dielectric loss ε'' vs frequency for 8CB confined to the molecular sieve M46 for $T=270.5$ K. The solid line is the whole fit function as a sum of two HN functions to the data. The dashed line presents the contribution of the surface layer and the dotted-dashed line the contribution of the molecules, which behave bulklike.

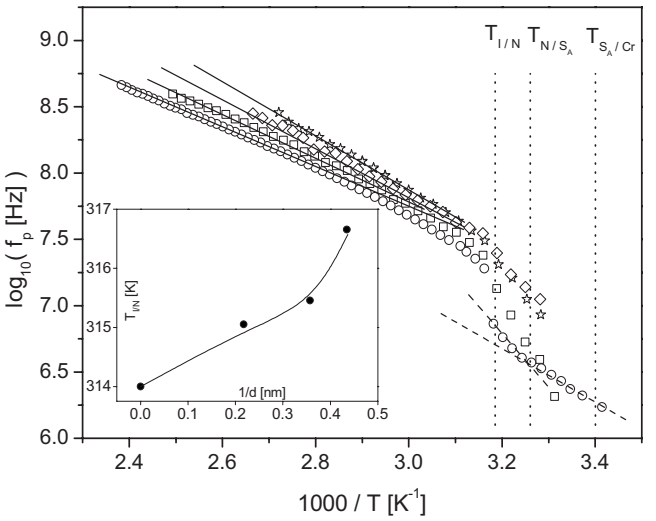

FIG. 6. Relaxation rate f_p versus $1/T$ for the relaxation process related to bulklike 8CB. ○: bulk 8CB; □: 8CB/M46; ◇: 8CB/M30; ☆: 8CB/M23. The solid lines are guides for the eyes. The dashed lines characterize the temperature dependencies of the relaxation rate of bulk 8CB in the nematic and smectic phase. The dotted lines indicate the phase transition temperatures of the bulk 8CB. The inset gives the estimated phase transition temperatures from the isotropic to the nematic phase versus inverse pore size. The line is a guide for the eyes.

isotropic state the temperature dependence of the relaxation rate of the process assigned to bulklike 8CB inside the pores is close to that observed for bulk 8CB. Its absolute values seem to be a bit higher and the transition from the liquid crystalline to the isotropic state is smeared out. This will be discussed in detail later. The process related to the fluctuation of 8CB molecules located in a surface layer is much slower than that of bulk 8CB. The temperature dependence of its relaxation rate seems to be curved when plotted versus $1/T$. In the following the peculiarities of each relaxation process are discussed separately.

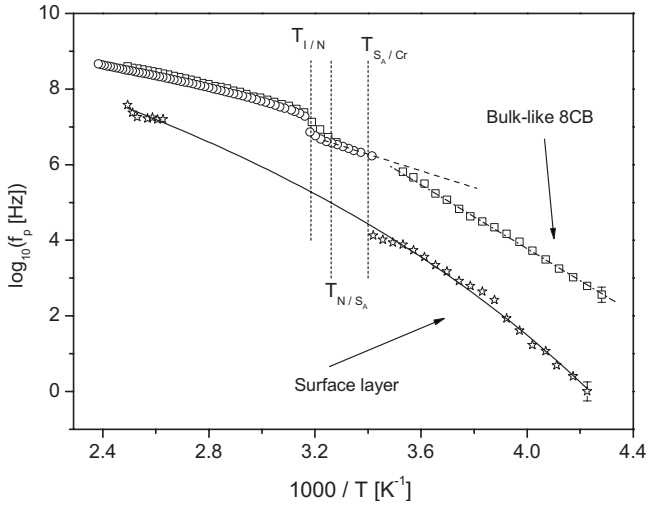

FIG. 5. Relaxation rate f_p vs $1/T$ for 8CB bulk (○) and for the different relaxation processes of the sample 8CB/M46. □: bulklike 8CB, ☆: surface layer. The dashed line characterizes the apparent activation energy of bulk 8CB in the smectic phase. The dashed dotted line characterizes the apparent activation energy of bulklike 8CB. The solid line is a fit of the VFT equation to the data of the surface layer (for details see text). The short dotted lines indicate the phase transition temperatures of bulk 8CB. The typical error is given by bars.

A. Relaxation process of bulklike 8CB

The high frequency relaxation processes observed for 8CB confined to the molecular sieves shows a close similarity with the behavior of bulk 8CB. Especially at the phase transitions temperatures of bulk 8CB changes in the temperature dependence of the relaxation rates of the high frequency process are also observed. This means that these molecules form liquid crystalline mesophases and can undergo phase transitions even when confined to the smallest pores of 2.3 nm. Therefore this process is assigned to 8CB in the center of the pores, which behaves bulklike. Figure 6 compares the temperature dependence of the relaxation rates of bulklike 8CB for different pore sizes. It becomes also clear from that figure and also from Fig. 5 that this bulklike relaxation process is modified by the confinement. In the isotropic state the values of the relaxation rates are higher than those for bulk 8CB and moreover its temperature dependence seems to be different.

In a first approach the Arrhenius equation (2) can be fitted to the data for the temperatures above the clearing temperature ($T_{I/N}$). The values of the estimated apparent activation energy increases systematically with decreasing pore size (see Fig. 7). This increase reflects the influence of the geometrical constraint on the molecular fluctuation in the isotro-

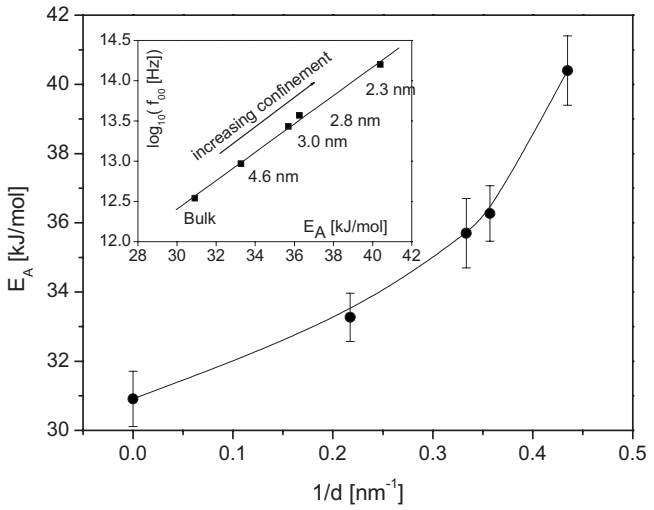

FIG. 7. Apparent activation energy E_A of the bulklike process in the isotropic state versus inverse pore size. The solid line is a guide for the eyes. The error bars result from the linear regression. The inset gives the correlation of $\log_{10} f_\infty$ and E_a in the compensation plot. The line is a linear regression to the data.

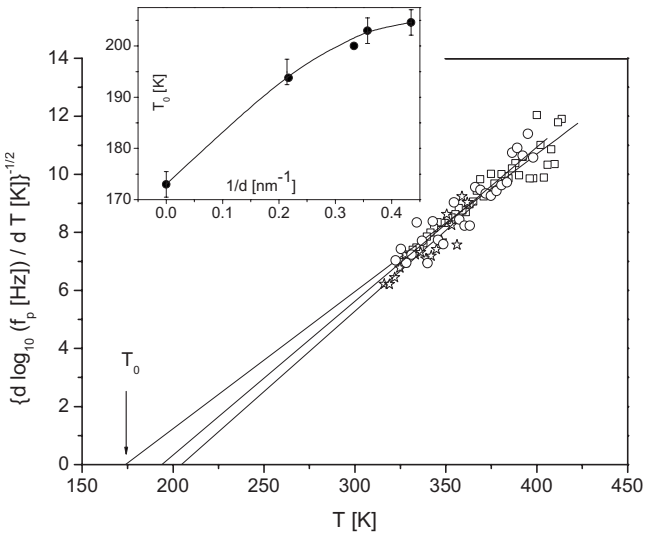

FIG. 8. $(d \log_{10} f_p/dT)^{-1/2}$ versus temperature for the bulklike process. ○: bulk 8CB; □: 8CB/M46; ☆: 8CB/M23. Lines are linear regressions to the data. The inset gives the Vogel temperature versus inverse pore size. The line is a guide for the eyes. The error bars result from the linear regression.

pic state. Probably the energy landscape of the bulklike fluctuations is modified by the geometrical confinement systematically and the energy barriers are increased. In addition the molecules, which behave bulklike, are influenced by the paranematic potential due to the surface layer, which also exists at temperatures above the clearing temperature of bulk 8CB.

A close inspection of the data especially for bulk 8CB shows that the data do not really follow a straight line when plotted versus $1/T$. In order to analyze the temperature dependence of the relaxation rates in more detail, a derivative technique was applied for temperatures above the clearing temperature ($T_{I/N}$). This method was previously described in detail [10,18,20(d)]. In brief for the VFT equation

$$\left(\frac{d \log_{10} f_p}{dT}\right)^{-1/2} = A^{-1/2}(T - T_0) \tag{4}$$

holds. Hence in a plot of $(d \log_{10} f_p/dT)^{-1/2}$ versus T a dependence according to the VFT equation shows up as a straight line. The Vogel temperature can be calculated from the condition $(d \log_{10} f_p/dT)^{-1/2}=0$. Figure 8 gives $(d \log_{10} f_p/dT)^{-1/2}$ versus T for different samples. First for all cases the data have to be described by a straight line, which indicates that the temperatures dependence of the relaxation rates of the bulklike relaxation process obeys the VFT law. This is expected because for temperatures higher than $T_{N/I}$ 8CB should behave as an ordinary glass forming liquid where such a behavior is known [20(d)]. Generally it is believed that VFT-like temperature dependence reflects the cooperative character of the underlying motional process. Secondly the estimated Vogel temperatures increases with decreasing pore size (see inset of Fig. 8). For the smallest pores size T_0 is more than 20 K higher than that of the bulk, which indicates a strong size effect. This is not known for ordinary glass forming liquid confined to nanoporous glasses such as salol embedded in nanoporous sol gel glasses [20(e)]. For the latter case at high temperature all data collapse into one chart independently of the pore size. Therefore, it is concluded that extra effects in addition to the confinement must take place for the confined 8CB. The difference between ordinary confined glass forming liquid and materials which can form liquid crystalline structure is the adsorbed surface layer with a paranematic order which gives rise to a paranematic potential. So this increase of T_0 may indicate that due to the confinement and probably more important to the paranematic potential of the surface layer the bulklike molecules are forced to fluctuate more cooperatively than in the bulk. With decreasing pore size the influence of the paranematic potential becomes more and more significant.

In the inset of Fig. 7 the pre-exponential factor $\log_{10} f_\infty$ is plotted versus the apparent activation energy. First, with decreasing pore size the $\log_{10} f_\infty$ increases and correlates linearly with E_A. This is an expression of the compensation law [28,29] and indicates again the cooperative nature of the motional process. This is in full agreement with the discussion of the increase of the Vogel temperature with decreasing pore size.

At the phase transition from the nematic to the smectic state of bulk 8CB the temperature dependence of the relaxation rates changes due to a change in the nematic potential (see Fig. 6). In both narrow liquid crystalline phase $f_p(T)$ can be approximated an Arrhenius law with apparent activation energies of 64.3 kJ/mol (nematic) and 43.5 kJ/mol (smectic). For the relaxation process due to bulklike 8CB molecules inside the pores a pronounced change in the temperature dependence of the relaxation rates close to $T_{N/I}$ of bulk 8CB can be observed. From the change in the temperature of the relaxation time a clearing temperature for the 8CB, which behave bulklike inside the pores, can be estimated (see inset Fig. 6). With decreasing pore size the clearing

temperature increases slightly. For simple liquids, which crystallize when confined to nanopores a freezing point, depression is observed. Also the magnitude of the effect ($\Delta T \approx 3$ K) is rather small in comparison to freezing point depression of simple liquids ($\Delta T \approx 10-20$ K) [4,30,31]. Obviously the Gibbs-Thomson equation also does not hold. This seems to indicate that surface tension effects do not play an important role.

At the phase transition temperature from the nematic to the smectic state $T_{S/N}$ of bulk 8CB the temperature dependence of the relaxation rate of the bulklike process does not show a pronounced change. That might indicate that the 8CB molecules, which behave bulklike inside the pores, do not undergo the phase transition form the nematic to the smectic state. Moreover, the bulklike relaxation process can be also observed for temperatures below $T_{Cr/S}$ where bulk 8CB crystallizes. This means that the formation of structures of with a higher order than a nematic phase of bulklike 8CB within the pores is frustrated by the confinement. One may further assume that the molecules which behave bulklike are influenced by a paranematic potential due to the surface layer even at temperatures corresponding to the smectic A and the crystalline state as well. Thus the formation of antiparallel molecular aggregates, normally existent in the smectic A state (Urban *et al.*, cited in Ref. [22]) or in the more ordered crystalline structures is suppressed in addition to purely geometrical restrictions also by the presence of the surface layer which results from the interaction of the 8CB molecules with the pore surface. The temperature dependence of the relaxation rates below the clearing temperature can be described by an Arrhenius law (see Fig. 5). The estimated values are in the range of 80 to 90 kJ/mol. These values are essentially higher than the values of the apparent activation energy in the smectic and nematic phase of bulk 8CB. This can be discussed in two directions. On the one hand, one can speculate that in confinement the geometrical restriction in combination with the paranematic potential increase the apparent activation energy of the molecular fluctuation of the bulklike 8CB molecules. On the other hand, it is known that the temperature dependence of the δ relaxation in the mesophase follows the VFT dependence if crystallization can be avoided [20(d)] in both the isotropic and the liquid crystalline state [21,24–27]. Here the crystallization is suppressed by the confinement. Therefore it is concluded that the high apparent activation energies found below $T_{Cr/S}$ are an expression of the underlying VFT-like temperature dependence.

B. Relaxation process of 8CB molecules forming the surface layer

As it is stated above, the relaxation of the process assigned to the molecular fluctuations of 8CB in a surface layer is essentially lower than that of the δ relaxation of bulk 8CB (see Fig. 5). FTIR measurements confirmed that the confined 8CB molecules interact strongly with pore walls by hydrogen bonding. Consequently, the molecular mobility of these molecules on the surface is strongly reduced compared to the bulk state. Figure 9 compares the temperature dependence of the relaxation rate of the surface layer for the different

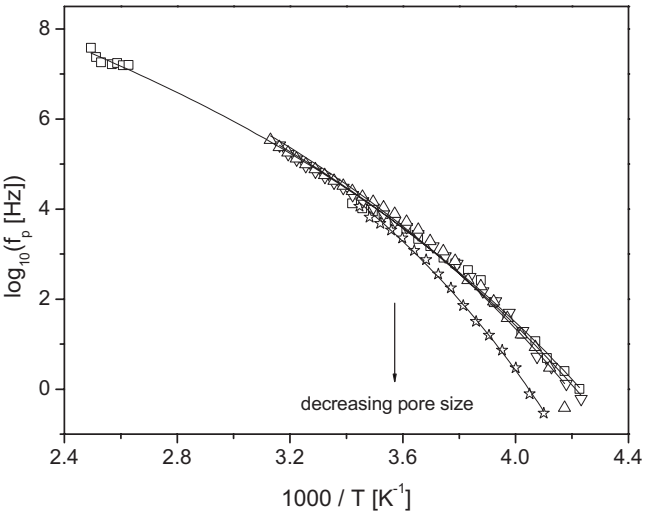

FIG. 9. $\log_{10} f_p$ versus inverse temperature for the process related to the surface layer. □: 8CB/M46; ▽: 8CB/M36; △: 8CB/M28; ☆: 8CB/M23. Lines are fits of the VFT equation to the data. The typical error in $\log_{10} f_p$ is ± 0.15. Error bars are avoid for seek of clearness.

samples. In general, $f_p(T)$ seems to be curved when plotted versus $1/T$. As discussed previously this can be taken as a hint for glassy dynamics taking place in the surface layer [20(d)]. For high temperatures the curves for the different pore sizes seem to collapse into one chart. From this result one has to conclude that the most important fact for the dynamics of the 8CB molecules in the surface layer is their interaction with the pore wall. This interaction slows down the molecular dynamics of the adsorbed molecules. But at lower temperatures the temperature dependence of the relaxation rate depends on the pore size (see Fig. 9). For smaller pore sizes $f_p(T)$ seems to be more curved than for larger ones. To analyze the data in more detail the VFT equation (3) is fitted to the data. Because for high temperatures all data collapse in to one curve the preexponetial factor $\log_{10} f_\infty$ is kept constant for all pore sizes. All fit parameters are given in Table III.

This analysis shows that the Vogel temperature T_0 related to the dynamics of the surface layer increase systematically with decreasing pore size (see Fig. 10). This increase in T_0 reflects in addition to the interaction of the molecules with the surface, the influence of the confining geometry on the molecular dynamics of the surface layer. With decreasing

TABLE III. VFT parameters of the process due to 8CB molecules forming the surface layer.

Sample	$\log_{10}(f_p[\mathrm{Hz}])$	A [K]	T_0 [K]	D	References
8CB/M23	11.7	931	167.8	2.41	This work
8CB/M28	11.7	1034	150.7	2.98	This work
8CB/M38	11.7	1085	145.0	3.25	This work
8CB/M46	11.7	1114	141.5	3.42	This work
$8CB/A_{380}$	14.3	2416	37.5	27.9	[18]

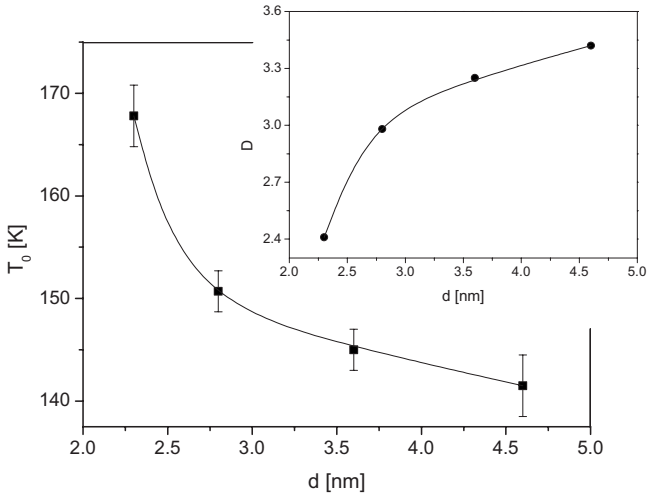

FIG. 10. Vogel temperature T_0 versus pore size d for relaxation process assigned to the surface layer. The line is a guide for the eye. The error bars results from the linear regression. The inset gives the corresponding fragility parameter D versus pore size. The line is a guide for the eyes.

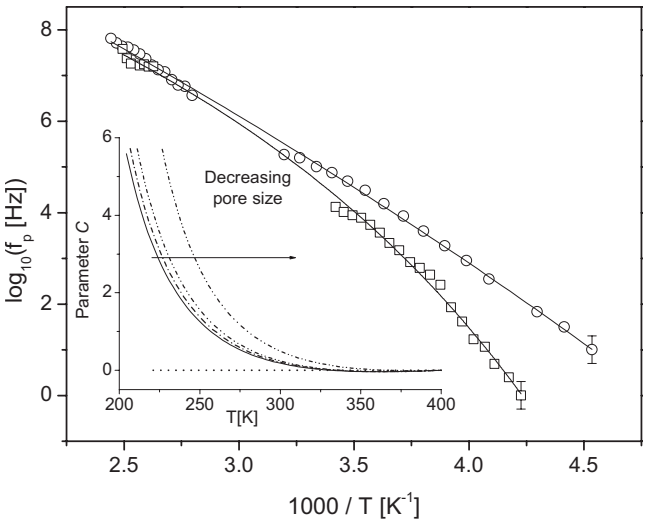

FIG. 11. $\log_{10} f_p$ versus inverse temperature for the process related to the surface layer for 8CB confined to M46 (□) and 8CB adsorbed onto aerosil A380 (○). The data for the latter are taken from Ref. [12]. Some typical error bars are given in the figure. The lines are fits of the VFT equation to the data. The inset gives the cooperativity parameter versus temperature for the different pore sizes.

pore size due to the geometrical constraint the molecular fluctuations of the molecules becomes more complicated with decreasing pore size reflected by an increase of T_0.

In addition to T_0 the so-called fragility is an important measure to characterize glassy dynamics. It describes the degree of the deviation from an Arrhenius-type temperature dependence [32]. Materials are called "fragile" if their $f_p(T)$ dependence deviates strongly from an Arrhenius-type behavior and "strong" if $f_p(T)$ is close to the latter. Despite the other possibilities the parameter $D=A/[T_0 \ln(10)]$ can be used as quantitative measure of fragility. D is calculated from the VFT parameters and plotted versus pore size in the inset of Fig. 10. D decreases systematically with pore size. With decreasing pore size the dynamical behavior of the surface layer changes from more strong to more fragile.

To discriminate between confinement effects and surface interaction it might be useful to compare the temperature dependence of the relaxation rates of the surface layer of 8CB molecules confined to the molecular sieves and adsorbed nearly in a monolayer at silica spheres of aerosil [18]. Such measurements were performed for nanocomposites of cyanobiphenyl molecules and aerosil. To obtain nearly a monolayer of adsorbed cyanobiphenyl molecules high concentration of silica (silica:cyanobiphenyl=7:1) was selected. Figure 11 compares the temperatures dependence of the relaxation rate of the surface layer of 8CB embedded into M46 and adsorbed onto the surface of aerosil A_{380} (Degussa) which is also covered by OH groups as the pore walls of the molecular sieves. For high temperatures both data sets collapse into one chart. The relaxation rates for the quite different systems agree with regard of the absolute values and their temperature dependence. But for lower temperatures the data strongly deviate from each other. The temperature dependence for the relaxation rates of the surface layer of 8CB molecules confined to the molecular sieves is much more curved than that for the same molecules only adsorbed to a surface. In addition, the absolute values of f_p are much lower for 8CB confined inside the pores. Assuming that the temperature dependence of 8CB molecules adsorbed at the surface is mainly due to its interaction with the surface one has to conclude that the stronger temperature dependence of 8CB embedded into the molecular sieves is due to confinement effects. On the basis of this idea a confinement parameter C could be defined by considering the ratio of both relaxation rates

$$C = \log_{10} f_p(T)_{A_{380}} - \ln f_p(T)_{\text{molecular sieves}} + \Delta. \qquad (5)$$

Using the estimated VFT parameters C can be calculated in its temperature dependence for the different pore sizes (see inset Fig. 11). Δ is a small adjustable parameter to normalize the small differences in the temperature dependence at high temperatures ($\Delta \approx -0.1 \cdots 0.1$) to zero. According to its definition at high temperatures C is zero and approximately constant. In this temperature range the molecular dynamics of the 8CB molecules is mainly controlled by its interaction with the pore wall. With decreasing temperature C deviates from zero and increases strongly at low temperatures. This indicates the growing influence of the restricting geometry on the molecular dynamics of the 8CB molecules in the surface layer. The deviation of C from zero shifts to higher temperatures with decreasing pore size. This indicates that the confinement effects for smaller pores are stronger than for larger ones.

A further indication of the influence of the restricting geometry on the molecular dynamics came from the investigation of 8CB confined to another type of molecular sieve AlSBA-15 with different pore filling degrees [5d]. For a high filling degree the temperature dependence of the relaxation time is much stronger than for a low one. For the latter case the most important effect is the interaction of the molecules

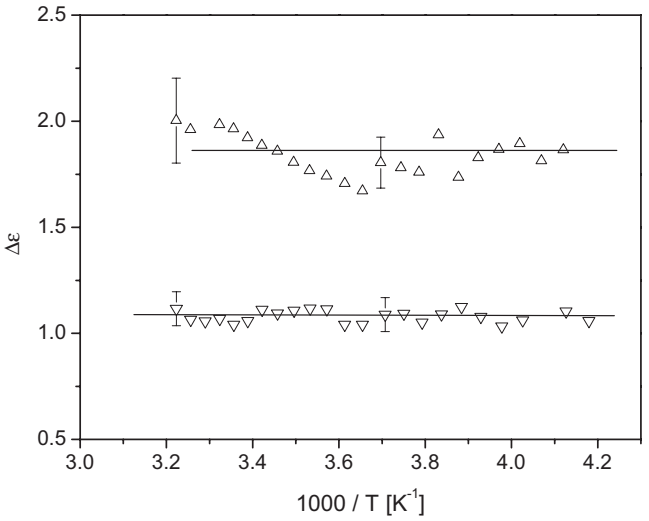

FIG. 12. Dielectric strength of the surface layer versus inverse temperature for samples with two different pores sizes. ▽: 8CB/M36; △: 8CB/M28. The lines are guides for the eyes. The error in $\Delta\varepsilon$ corresponds to the scatter of the data.

with the pore surface. The second surface layer is quasifree from this point of view. In the case of the pores with a high filling degree the bulklike material in the center of the pores is further constrained by the molecules located in the surface layer. This causes additional restrictions to its molecular fluctuations compared to that of a quasifree surface layer for the pores with a low filling degree.

To complete the discussion, the temperature dependence of the dielectric strength of the process will be discussed briefly. The Debye theory of dielectric relaxation generalized by Kirkwood and Fröhlich [20(d)] predicts for the temperature dependence of the dielectric relaxation strength

$$\Delta\varepsilon = \frac{1}{3\varepsilon_0} g \frac{\mu^2}{k_B T} \frac{N}{V}, \tag{6}$$

where μ is the mean dipole moment of the process under consideration and N/V is the number density of dipoles involved. g is the so-called Kirkwood-Fröhlich correlation factor, which describes static correlation between the dipoles. The Onsager factor describing internal field effects is omitted for sake of simplicity. Figure 12 gives the temperature dependence of $\Delta\varepsilon$ of the surface process for two different pore sizes as example. For the other pore sizes a similar behavior as that shown in Fig. 12 is observed. Figure 12 shows that $\Delta\varepsilon$ is approximately constant. According to Eq. (6) the relaxation strength should decrease with increasing temperature. So the temperature dependence of $\Delta\varepsilon$ is probably due to a counterbalance of two different effects. Thermal energy should lead to an in decrease of $\Delta\varepsilon$ with increasing temperature. But also with increasing temperature the strength of the interaction of the molecules with the surfaces decreases which should lead to an increase in $\Delta\varepsilon$ due an increased number of fluctuating dipoles or by an increase in its fluctuation angle. The experimental results show that both effects compensate each other.

A quantitative discussion of $\Delta\varepsilon$ in dependence of the pore size cannot be carried out because the measurements were done on pressed pellets of the powder of the molecular sieves. This means that the samples contain different amounts of extra voids due to the pressing. The amount of these extra voids is not known and therefore a correction of $\Delta\varepsilon$ for that cannot be done.

IV. CONCLUSIONS

The molecular dynamics of 8CB confined in AlMCM-41-type molecular sieves with identical structure and composition but a different pore sizes was investigated by broadband dielectric spectroscopy over a large frequency and temperature range. These measurements were accompanied by TGA analysis to obtain the filling degree and FTIR investigation to establish the interaction of the 8CB molecules with the pore surface via hydrogen bonding.

TGA data show that bulk 8CB and confined 8CB samples thermally decompose in a similar manner. The small difference between bulk and confined 8CB might indicate the interaction of the molecules with the surface in the composite systems. The quantitative analysis of TGA measurements leads to the conclusion that the calculated values of the filling degree are close to that expected for completely filled pores. The calculations were done assuming that the density of confined 8CB equals that of the bulk.

The dielectric spectra show in addition to conductivity and Maxwell-Wagner-Sillars effects two relaxation processes: a bulklike relaxation process, which is related to the molecules located in the pore center. The second relaxation process measured at essentially lower frequencies than the former one is assigned to molecules located in a surface layer, having a strong interaction with surface OH groups by hydrogen bonding as shown by FTIR spectra. There are indications that the adsorbed 8CB molecules have a paranematic structure at the surface induced by a paranematic potential.

The Arrhenius equation can be roughly fitted to the temperature dependence of the relaxation rate of the process related to bulklike 8CB for the temperature above the clearing temperature. The estimated apparent activation energy increases systematically with decreasing pore size: this shows the influence of the geometrical constraint and the paranematic potential due to the molecules in the surface layer on the molecular fluctuation in the isotropic state. In an alternative way the VFT equation is used to analyze this temperature dependence in more detail employing a derivative technique. This analysis shows that the Vogel temperature T_0 increase with decreasing pore size. Generally it is believed that a VFT behavior is related to the cooperative character of the underlying molecular motions. The increase of T_0 with decreasing pore size indicates that the molecules are forced to fluctuate more cooperatively due to the confinement and the paranematic potential of the surface layer than in the bulk. This argument is also supported by the linear dependence of the $\log_{10} f_\infty$ and E_A on pore size as expected from compensation law.

The phase transition for the isotropic to the nematic state is slightly shifted to higher temperatures by few degrees: this

indicates that the Gibbs-Thomson equation does not hold for the investigated system. Moreover it was shown that the formation of structures of with a higher order than a nematic phase of the bulklike 8CB within the pores is frustrated by the confinement as shown by the lack of a clear phase transition from nematic to smectic and further to crystalline state and probably the formation of antiparallel molecular aggregates is suppressed under confinement. High apparent activation energies are found for temperatures below $T_{Cr/S}$, which might by an expression of the underlying VFT-like temperature dependence found also in the mesophases of liquid crystals, which do not crystallize.

Also the temperature dependence of the relaxation rate of the process related to the molecules, which fluctuate in the surface layer, has to be described by the VFT equation. At high temperatures all data collapse into one chart where at lower ones the data depends on pore size. The corresponding Vogel temperature increases systematically by more than 25 K with decreasing pore size. The temperature dependence of the relaxation rate of the surface is due to two effects: the interaction of the 8CB molecules with the pore walls and the geometrical restriction due to confinement. At high temperatures mainly the interaction of the molecules with the surface dominates whereas at lower temperatures the spatial restriction due to the confinement becomes more and more important. To separate between the interaction of the molecules with the surface and the confinement effects the data of 8CB molecules forming a surface layer inside the pores are compared with the temperature dependence of the same molecules adsorbed in a nearly monolayer structure on the outer surface of silica spheres of aerosil. The latter is regarded as the case where the temperature dependence of f_p is only due to the interaction of the molecules with the surface. At high temperatures the temperature dependence of the relaxation rate of the surface of the different systems agrees with respect to both its absolute values and its temperature dependence. This result indeed justifies the assumption that at high temperatures the $f_p(T)$ of the surface layer is controlled mainly by the interaction of the molecules with the surface. For low temperatures $f_p(T)$ is strongly different for both systems. For 8CB confined inside the pores the relaxation rate is much lower and $f_p(T)$ is more curved when plotted versus $1/T$. This indicates the growing influence of the confinement on the molecular fluctuation of the 8CB forming the surface layer. On this basis a confinement parameter is defined and discussed in dependence of the pore size.

The temperature dependence of the dielectric strength of the process due to the surface layer is found to be almost constant despite the decrease predicted by Debye theory of dielectric relaxation (generalized by Kirkwood and Fröhlich). This is probably due to the competition of two or more effects, such as an increased number density of fluctuating dipoles or an increase in its fluctuation angle due to decreased interaction of the molecules with the surface with increasing temperature.

ACKNOWLEDGMENTS

L.F. and S.F. thank the financial support of Romanian Ministry of Education and Research (COMAFI Core Program). The financial support of S.F. and L.F. and the logistic support from the Federal Institute of Materials Research and Testing (BAM) as well as the samples supplied by Berlin Branch of Leibniz Institute of Catalysis (Dr. Irene Pitsch technically assisted by Margret Buddrus) are gratefully acknowledged.

[1] *Molecular Dynamics in Restricted Geometries*, edited by J. Klafter and J. Drake (Wiley, New York, 1989); *Dynamics in Small Confining Systems*, edited by J. Drake, J. Klafter, P. Levitz, R. Overney, and M. Urbach MRS Symp. Proc. No. 651 (Materials Research Society, Pittsburgh, 2001).

[2] *Access in Nanoporous Materials*, edited by T. J. Pinnavaia and M. F. Thorpe (Plenum Press, New York, 1995).

[3] *Liquid Crystals in Complex Geometries Formed by Polymer and Porous Networks*, edited by G. P. Crawford and S. Zumer (Taylor and Francis, London, 1996).

[4] *International Workshop on Dynamics in Confinement*, edited by R. Zorn, B. Frick, and H. Büttner [J. Phys. IV **10**, **Pr7** (2000)]; *Proceedings of the 2nd International Workshop on Dynamics in Confinement*, edited by B. Frick, M. Koza, and R. Zorn [Eur. Phys. J. E **12**, 1 (2003)]; *Proceedings of the 3rd International Workshop on Dynamics in Confinement*, edited by M. Koza, B. Frick, and R. Zorn [Eur. Phys. J. Spec. Top. 141, 3 (2007)].

[5] T. Bellini, M. Buscaglia, C. Chiccoli, F. Mantegazza, P. Pasini, and C. Zannoni, Phys. Rev. Lett. **85**, 1008 (2000).

[6] H.-L. Zubowa, H. Kosslick, E. Carius, S. Frunza, L. Frunza, H. Landmesser, M. Richter, E. Schreier, U. Steinike, and R. Fricke, Microporous Mesoporous Mater. **21**, 467 (1998).

[7] S. Frunza, A. Schönhals, L. Frunza, H.-L. Zubowa, H. Kosslick, R. Fricke, and H. Carius, Chem. Phys. Lett. **307**, 167 (1999); S. Frunza, L. Frunza, and A. Schönhals, J. Phys. IV **10**, Pr7–115 (2000).

[8] I. Gnatyuk, G. Puchkovskaya, O. Yaroshchuk, Y. Goltsov, L. Matkovskaya, J. Baran, T. Morawska-Kowal, and H. Ratajczak, J. Mol. Struct. **511-512**, 189 (1999); T. Gavrilko, I. Gnatyuk, G. Puchkovskaya, Yu. Goltsov, L. Matkovskaya, J. Baran, M. Drozd, and H. Ratajczak, Vib. Spectrosc. **23**, 199 (2000); I. Gnatyuk, T. Gavrilko, G. Puchkovska, I. Chashchnikova, J. Baran, and H. Ratajczak, J. Mol. Struct. **614**, 233 (2002).

[9] L. Frunza, H. Kosslick, U. Bentrup, I. Pitsch, R. Fricke, S. Frunza, and A. Schönhals, J. Mol. Struct. **651-653**, 341 (2003); L. Frunza, S. Frunza, I. Enache, T. Beica, A. Schönhals, H. Kosslick, U. Bentrup, and I. Pitsch, Mol. Cryst. Liq. Cryst. **418**, 69 (2004).

[10] L. Frunza, H. Kosslick, S. Frunza, and A. Schönhals, Microporous Mesoporous Mater. **90**, 259 (2006).

[11] M. D. Dadmun and M. Muthukumar, J. Chem. Phys. **98**, 4850 (1993).

[12] X. Wu, W. I. Goldburg, M. X. Liu, and J. Z. Xue, Phys. Rev. Lett. **69**, 470 (1992).
[13] G. P. Sinha and F. M. Aliev, Phys. Rev. E **58**, 2001 (1998).
[14] C. T. Kresge, M. E. Leonowicz, W. J. Roth, J. C. Vartuli, and J. S. Beck, Nature (London) **359**, 710 (1992); J. S. Beck, J. C. Vartuli, W. J. Roth, M. E. Leonowicz, C. T. Kresge, K. D. Schmidt, C. T-W. Chu, D. H. Olson, E. W. Sheppard, S. B. McCullen, J. B. Higgins, and J. C. Schlenker, J. Am. Chem. Soc. **114**, 10834 (1992).
[15] H. Kosslick, I. Mönnich, E. Paetzold, G. Oehme, and R. Fricke, Microporous Mesoporous Mater. **44–45**, 537 (2001); I. Pitsch, U. Kürschner, D. Müller, B. Parlitz, E. Schreier, R. Trettin, R. Bertram, and W. Gessner, J. Mater. Chem. **7**, 2469 (1997).
[16] L. Frunza, A. Schönhals, H. Kosslick, and S. Frunza, Eur. Phys. J. E **26**, 379 (2008).
[17] G. S. Iannachione, C. W. Garland, J. T. Mang, and T. P. Rieker, Phys. Rev. E **58**, 5966 (1998).
[18] S. Frunza, L. Frunza, A. Schönhals, H. Sturm, and H. Goering, Europhys. Lett. **56**, 801 (2001); S. Frunza, L. Frunza, M. Tintaru, I. Enache, T. Beica, and A. Schönhals, Liq. Cryst. **31**, 913 (2004).
[19] S. Frunza, H. Kosslick, A. Schönhals, L. Frunza, I. Enache, and T. Beica, J. Non-Cryst. Solids **325**, 103 (2003).
[20] *Broadband Dielectric Spectroscopy*, edited by F. Kremer and A. Schönhals (Springer-Verlag, Berlin, 2003), (a) p. 35; (b) p. 59; (c) p. 392; (d) p. 99; (f) p. 171.
[21] S. Urban, B. Gestblom, H. Kresse, and A. Dabrowski, Z. Naturforsch., A: Phys. Sci. **51**, 834 (1996).
[22] A. Schönhals, H.-L. Zubowa, R. Fricke, S. Frunza, L. Frunza, and R. Moldovan, Cryst. Res. Technol. **34**, 1309 (1999).
[23] J. Jadzyn, G. Czechowski, R. Douali, and C. Legrand, Liq. Cryst. **26**, 1591 (1999).
[24] H. R. Zeller, Phys. Rev. Lett. **48**, 334 (1982).
[25] L. Benguigui, Phys. Rev. A **28**, 1852 (1983); **29**, 2968 (1984); Mol. Cryst. Liq. Cryst. **114**, 51 (1984).
[26] A. C. Diogo and A. F. Martins, J. Phys. (Paris) **43**, 779 (1982).
[27] A. R. Brás, M. Dionísio, H. Huth, Ch. Schick, and A. Schönhals, Phys. Rev. E **75**, 061708 (2007).
[28] J. C. Dyre, J. Phys. C **19**, 5655 (1986).
[29] A. Yelon, B. Movaghar, and H. M. Brantz, Phys. Rev. B **46**, 12244 (1992).
[30] H. K. Christenson, J. Phys.: Condens. Matter **13**, R95 (2001), and references herein.
[31] C. Alba-Simionesco, B. Coasne, G. Dosseh, G. Dudziak, K. E. Gubbins, R. Radhakrishnan, and M. Sliwinska-Bartkowiak, J. Phys.: Condens. Matter **18**, R15 (2006), and the references herein.
[32] C. A. Angell, J. Non-Cryst. Solids **13**, 131 (1991); J. Res. Natl. Inst. Stand. Technol. **102**, 171 (1997).